Investigating the potential benefit to a mesoscale NWP model of a microwave sounder on board a geostationary satellite

Fabrice Duruisseau, Philippe Chambon, Stephanie Guedj, Vincent Guidard, Nadia Fourrié, Françoise Taillefer, Pierre Brousseau, Jean-Francois Mahfouf, Rémy Roca

Investigating the potential benefit of a Microwave sounder on-board a geostationary satellite on Numerical Weather Prediction with a meso-scale model

Fabrice Duruisseau[(1)], Philippe Chambon[(1)*], Stéphanie Guedj[(1)+], Vincent Guidard[(1)], Nadia Fourrié[(1)], Françoise Taillefer[(1)], Pierre Brousseau[(1)], Jean-François Mahfouf[(1)] and Rémy Roca[(2)]

(1) CNRM UMR 3589, Météo-France/CNRS, Toulouse, France

(2) LEGOS, OMP, Toulouse, France

* Correspondence to: P. Chambon, CNRM UMR 3589, Météo-France/CNRS, 42 avenue Gaspard Coriolis, 31057, Toulouse Cedex, France. Email: philippe.chambon@meteo.fr

+ Present affiliation: Joint Center for Satellite and Data Assimilation, College Park, Maryland, USA

Abstract

Observing the Earth with a microwave radiometer on-board a geostationary satellite has generated interest for several decades. Such a mission would add a high observation rate in the microwave spectrum, offered by a geostationary orbit, to the sounding capabilities of the current observing system. The instrumental concept under study considers a microwave radiometer with six channels with different observation errors within the 183.31 GHz water vapour absorption band.

Observing System Simulation Experiments (OSSEs) are conducted to examine if these very frequent microwave observations would be beneficial to mesoscale numerical weather prediction (NWP) and complement the current or soon-available satellite observations. The OSSE framework is built up on (i) simulated observations from a known "truth" which is a long and uninterrupted forecast from the Météo-France ARPEGE global model, and (ii)

This article has been accepted for publication and undergone full peer review but has not been through the copyediting, typesetting, pagination and proofreading process, which may lead to differences between this version and the Version of Record. Please cite this article as doi: 10.1002/qj.3070

the Météo-France AROME meso-scale model in which the simulated observations are assimilated using a 1 hour update cycle 3D-Var data assimilation system.

Benefits that may be expected from such a microwave sounder mission are evaluated in the context of a dense observing system including observations from the future hyper-spectral Infra-Red Sounder on board Meteosat Third Generation. In particular, impacts of microwave observations with observation errors ranging from 1.25 K to 5 K are studied. One of the main findings of this study is that fine-scale NWP systems do not only need observations that are frequent in space and time, but that these observations must be accurate as well.

1. Introduction

The possibility of a radiometer observing the Earth in the microwave spectrum from a geostationary earth orbit (GEO) has been long studied (e.g. El Raey, 1982). Such a mission would add the high observation rate offered from GEO to the sounding capability of the current observing system. Several instrument concepts using different technologies paved the way for future investigations (e.g. Bizzarri, 2000; Bizzarri *et al.*, 2002; Gasiewski *et al.*, 2003). While pioneering projects like GOMAS (Geostationary Observatory for Microwave Atmospheric Sounding; Bizzarri, 2000) were based on sounding technologies similar to the ones used for Low Earth Orbiting satellites, the latest studies are focused toward synthetic aperture interferometric radiometry (Martín-Neira *et al.*, 2014). Active research is on-going on this subject with several concepts under investigation: the GeoSTAR (Geostationary Synthetic Thinned Aperture Radiometer) and the GeoMAS (Geostationary Millimeter-wave Array Spectrometer) instruments on-board the PATH (Precision and All-Weather Temperature and Humidity) mission under study in the United States (e.g. Tanner *et al.*, 2006; Lambrigtsen *et al*., 2007; Gaier *et al*., 2011; Blackwell *et al.*, 2011; Austerberry *et al*., 2015), the GAS (Geostationary Atmospheric Sounder) instrument under study in Europe for post-Meteosat Third Generation satellites (e.g. Christensen *et al*., 2007; Carlström *et al*., 2009; Camps *et al*., 2016a; Camps *et al*., 2016b), the GIMS (Geostationary Interferometric Microwave Sounder) instrument under study for possible implementation in the framework of the Chinese Fēngyún geostationary satellite series FY-4 (Liu *et al*., 2009; Liu *et al*., 2011; Zhang *et al*., 2012; Chen *et al*., 2015; Li *et al*., 2015; Zhang *et al*., 2015a; Zhang *et al*., 2015b).

The present study was sponsored by the European Space Agency (ESA) in order to bring a data user perspective to the microwave geosounder concept and evaluates the potential benefit of such an instrument for fine-scale Numerical Weather Prediction (NWP) by conducting Observing System Simulation Experiments (OSSEs, e.g. Wang *et al*., 2013; Privé *et al*., 2014; Guedj *et al*., 2014; Atlas *et al*., 2015; Hoffman and Atlas, 2016; Ma *et al*., 2015).

The mission concept under investigation in this paper includes observations with different observation errors, within the 183.31 GHz water vapour absorption band. This frequency band is a preferred choice for such an instrument since high microwave frequencies overcome the limitations due to spatial resolution from a geostationary platform (e.g. Prigent *et al.*, 2006). The present paper is focused on the impact of 183.31 GHz observations on humidity and precipitation forecasts in the context of a future much more mature observing

system. This system will include a new generation of GEO hyperspectral infrared atmospheric sounders providing accurate temperature and water vapour soundings with high temporal frequency. Currently planned instruments of this class include the GIIRS (Geostationary Interferometric Infrared Sounder) instrument on-board the future Chinese FY-4 satellites series and the IRS (Infra-Red Sounder) on-board the European Meteosat Third Generation-Sounder series.

The paper is organized as follows: the OSSE framework and each of its components are detailed in Section 2. The experiment design as well as the methods used for the impact evaluation on humidity and precipitation forecasts are described in Section 3. Experimental results are summarized in Section 4. A summary, as well as conclusions and a description of the limitations of applicability of the results are given in Section 5.

2. Observing System Simulation Experiment framework

2.1 General Framework

OSSE frameworks have been developed in several research facilities and NWP centres. The basic principle of an OSSE is to assimilate synthetic observations derived from an atmospheric model state assumed to represent the truth, and then to determine the impact on analyses and forecasts. The more realistic each of the OSSE components is, the more consistent the results will be with experiments using real observations. In particular, the large expertise in the development and validation of OSSEs at NASA GMAO and NCEP (e.g. Errico *et al*., 2007; Masutani *et al*., 2010; McCarty *et al*., 2012; Errico *et al*., 2013; Privé *et al*., 2013a; Privé *et al*., 2013b; Boukabara *et al*., 2016) helped formulating recommendations for future realistic OSSEs, some of which are considered in this paper and described below.

Guedj *et al*. (2014) developed an OSSE framework to assess the potential impact of the Infrared Sounder (IRS) instrument on the Météo-France mesoscale numerical weather predictions over Western Europe. The OSSEs carried out in this study follow the same methodology with enhanced simulation of the impact of clouds on the use of radiance observations and a new calibration of observation errors. It corresponds to the framework shown on Figure 1:

- The reference atmospheric state or “Nature Run”, from which observations are simulated, is described in Section 2.2

- The numerical weather prediction model and data assimilation system, which are used for generating the analyses and forecasts are then described in Section 2.3.
- The simulation of the different observations, including those from a future/hypothetical geostationary microwave sounder, are detailed in Section 2.4.

2.2 Nature Run: the ARPEGE global model

The numerical model used for the generation of a reference ("true") atmospheric state or Nature Run (NR) is the French spectral global model ARPEGE (Action de Recherche Petite Echelle Grande Echelle), operational at Météo-France since 1992 (Courtier *et al*., 1991). The spectral resolution is T1198 with a stretched and tilted grid (Courtier and Geleyn, 1988), which corresponds to a horizontal resolution ranging from 7 km over Europe to 40 km over the Antipodes.

The NR used here is a two-month long ARPEGE forecast, initialized with the operational ARPEGE 4D-Var analysis from June 1st, 2015 at 00 h UTC. Model outputs saved every hour have been used to simulate all the synthetic observations described below as well as to compute forecast skill scores.

Realistic lower boundary conditions over oceans are specified by the daily sea surface temperature forcing from OSTIA analyses (Operational Sea Surface Temperature and Sea Ice Analysis; Stark *et al*., 2007).

2.3 Data assimilation system: the AROME regional model

The NWP model used for conducting the OSSEs is the convective scale AROME-France model that has been running operationally at Météo-France since 2008 (Seity *et al*., 2011). The model domain covers Western Europe (see Figure 4) with a 2.5 km horizontal resolution and 60 vertical levels, corresponding to resolutions lower than the current operational set up (1.3 km horizontal resolution with 90 vertical levels since April 2015).

The AROME forecasts are initialized using analyses from a 3D-Var data assimilation system with 1-hour cycling (Brousseau *et al*., 2016), which can take advantage of the frequent observations provided by geostationary satellites. Perfect lateral boundary conditions as well as perfect sea surface temperature are provided by the NR. Regarding lateral boundary conditions, an alternative solution would have been to run a global OSSE first from which boundary conditions for the regional OSSEs could be derived. This approach was developed by Atlas et

al. (2015) to run regional OSSEs experiments focused on hurricane forecasting and may be considered in our future OSSEs.

The AROME model is a state-of-the-art non-hydrostatic dynamical model (Bubnova *et al.*, 1995) with an explicit description of moist convection (Seity *et al.*, 2011). These main features are rather different from the configuration of the ARPEGE model used to generate the NR - hydrostatic dynamical model core and parameterized moist convection (Bougeault, 1985). Hence, using this model for the data assimilation and forecast components in the OSSE system avoids the so-called "identical twin" problem that can result in overly optimistic OSSE impact results (e.g. Masutani *et al*., 2010). We limit the OSSE time period to 1 month since running such a system requires large computational resources, especially so when using a 1 h data assimilation cycling.

2.4 Simulation and calibration of a synthetic Observing System

Observations are simulated from the NR over the AROME domain. The current (2015) observing system is described in Section 2.4.1 and the future/hypothetical geostationary observations are described in Section 2.4.2.

2.4.1 Simulation and calibration of current observations

Observations used in the operational AROME data assimilation system include a wide variety of measurements in two general categories: the conventional observations (radiosoundings, aircraft measurements, land stations...) and the radiances (or the equivalent brightness temperatures) provided by satellite observing systems which are simulated using the radiative transfer model RTTOV V10 (https://nwpsaf.eu/). Types of conventional and satellite observations that are used are listed in Table 1 and the number of observations of each type was assimilated within the experiments detailed in the next section is shown on Figure 2. Of all the observations assimilated in AROME in operations, only the ground radar data are not included in the OSSE system (Wattrelot *et al*., 2014). The reason for this is because the cloud and precipitation schemes used for the ARPEGE and AROME models are very different and the observation operator used to simulate radar reflectivities was specifically designed for cloud resolving models (Caumont *et al.*, 2006).

Synthetic observations have been generated through several steps: (i) the geographical locations of actual observations are taken as the locations of the simulated observations to ensure a realistic sampling of the atmosphere from the NR for most of the observations, except for AMVs which are kept at the location of real cloudy scenes but do not necessarily correspond to cloudy scenes in the NR, (ii) the observations operators from the operational AROME 3D-Var system are applied to the NR atmospheric columns, at the observations locations, and (iii) Gaussian random and uncorrelated perturbations are added to each synthetic observation. It is likely that correlated errors would improve the realism of the simulated observations and their impact, especially since the AROME data assimilation system cannot take into account non-diagonal observation error covariance matrices yet.

A critical step when setting up an OSSE concerns the calibration of the standard deviations of the explicitly added observation errors. In the present configuration, they are initially taken to be the estimated observation errors that are specified in the AROME 3D-Var system. Further calibration is required to ensure that each observing system has a realistic impact on analyses and forecasts as explained below.

The OSSE calibration was performed as an iterative process during which the variances of observation errors are been tuned for each observation type so that the first guess departures within the OSSEs converge toward comparable first guess departures in reality with actual observations. A good agreement between first guess departures from the OSSE and from a real data assimilation system is an indicator of the realism of the OSSE framework. This is critical since the simulated observation errors propagate through the 3D-Var system and then nonlinearly in time by the atmospheric model.

The calibration iterative process was performed following Errico et al. (2013):

- a first 1 h cycling data assimilation experiment was ran over a 10-day period, with all the synthetic observations mentioned above randomly perturbed using initial observation errors as assigned to real observations in the AROME operational framework.
- the standard deviations of first guess departures from this initial experiment was then compared to their counterpart with real observations to estimate a revised set of standard deviations for each observation type.

- a revised set of synthetic observations was then created with perturbations adjusted to match the revised standard deviations.
- the 1 h cycling data assimilation experiment was run again over a 10-day period with the revised synthetic observations and the same process was then repeated until OSSE first guess departure standard deviations converge toward the reference ones.

Calibration results after fifteen iterations of 10-day 1 h cycling are presented on Figure 3 for nine observing systems, showing a good agreement between the synthetic and real observations of the OSSEs main observing systems in terms of standard deviation of first guess departures. Note the very good agreement that is obtained for winds, temperature and humidity observed by radiosondes and aircraft and for brightness temperatures observed by AMSU-A.

2.4.2 Simulation of future/hypothetical geostationary observations

2.4.2.1 Infra-Red Sounder on-board Meteosat Third Generation

Meteosat Third Generation is the next generation series of European operational geostationary satellites (Stuhlmann *et al*., 2005; Rodriguez *et al*., 2009; see also http://www.eumetsat.int/website/home/Satellites/FutureSatellites/MeteosatThirdGeneration/index.html). The sounding platform MTG-S, to be positioned at a longitude between 10ºE and 10ºW, will host the hyperspectral Infrared Sounder (IRS). IRS will provide information on atmospheric water vapour and temperature at an unprecedented temporal frequency over the full disk, covering Western Europe and Africa as well as the Atlantic Ocean, with 920 channels between 4.6 μm and 6.25 μm, and 800 channels between 8.3 μm and 14.3 μm.

As mentioned above, Guedj *et al*. (2014) performed various OSSEs in order to make a first assessment on the potential impact of this instrument with different experimental set-ups (channel selections, horizontal thinning). The configuration found best to improve the AROME forecasts has been chosen for the present study, with an improved simulation of the effect of quality control on cloud affected radiances implemented via a cloud screening methodology based on hydrometeor content form the NR (Section 2.5). This configuration consists of (i) a selection of 25 water vapour channels, listed in Table 2, which limits the inter-channel errors correlations since the current AROME 3D-Var assumes a diagonal observation error covariance matrix and (ii) a horizontal thinning of 80 km to avoid spatial error correlations. The observation errors applied to the IRS channels selection

have been estimated based on the calibrated estimates for the IASI and SEVIRI data (Guedj *et al*., 2014) and range from 0.45 K to 2 K. Simulated IRS observations are computed from the NR atmospheric profiles, using the RTTOV radiative transfer model.

It is likely that other Level 2 meteorological products will be derived from the IRS instruments, including Atmospheric Motion Vectors (AMVs) which may be characterized by smaller height assignment errors than current AMVs derived from current infrared imagers like SERIVI. However, since the assimilation of these future products has not been implemented in the AROME data assimilation system, this work is left for future OSSEs and only IRS Level 1 radiance data are considered in this paper.

2.4.2.2 A microwave sounder on-board a geostationary satellite

The microwave geostationary observations, that are the focus of this study are from a potential instrument (hereafter, MWGEO), sounding the atmosphere within the 183.31 GHz water vapour absorption band, with the same six channels as the SAPHIR instrument on-board the Megha-Tropiques satellite (Roca *et al*., 2015). This provides the best sampling of the 183.31 GHz absorption band compared to other similar available instruments (3 channels for AMSU-B and MHS, 5 channels for ATMS and MWHS-2). A list of the MWGEO channels is given in Table 3.

Several observation error magnitudes have been considered. The lowest observation error of 1.25 K corresponds to typical AMSU-B/MHS 183.31 GHz observations errors and results from the calibration process described in Section 2.4.1 (a value of 2 K is used in operations for the assimilation of AMSU-B/MHS 183.31 GHz channels). This 1.25 K observation error is considered as a baseline for Low Earth Orbiting (LEO) microwave sounders and the best observation error that a MWGEO could achieve; this configuration is referred to below as MWGEOx1.

Two other MWGEO configurations are then selected, with two-times and four-times larger error standard deviations. In the following, they are referred to as MWGEOx2 and MWGEOx4. According to Chen *et al*. (2015), who evaluated the capabilities of three different instrumental technologies for a MWGEO, a 5 K observation error standard deviation would be realistic for such an instrument and this value could potentially be decreased with longer signal integration time of the interferometer measurements. Hence, the selected MWGEO configurations cover the range of realistic scenarios in terms of potential observation errors.

The synthetic brightness temperatures from the three different MWGEO are simulated the same way as IRS measurements, with the RTTOV radiative transfer model applied to the NR atmospheric columns, and then perturbed with observation errors with the specified statistics. As can be seen in Figure 4, increasing observations errors lead to highly perturbed observations. Within the data assimilation experiments, these observations are horizontally thinned to a mean distance of 80 km as is done for the IRS observations and for the same reasons.

For the reasons mentioned for the MTG/IRS observing system, only potential Level 1 data of a MWGEO satellites are considered in this study. However, some Level 2 data like AMVs products derived from microwave observations might prove to be useful for NWP forecasts and could be considered in future OSSEs.

2.5 Quality control and synthetic observations

In the OSSE framework, regular quality controls such as "first-guess checks", ensuring that the difference between observation values and first guess values do not exceed the RMS of observation and background errors, are applied as in reality to all non-radiance observations. However, there is no contamination by clouds and precipitation in the synthetic observations since the RTTOV simulations are performed assuming clear sky conditions. Hence, a number of quality controls applied to real satellite radiances, in particular those based on window channels would not be effective here. For an OSSE, it is important that there is a realistic ratio of observations contaminated by clouds and precipitation for each sensor type. This is especially the case in the present set of experiments. Therefore, alternative methods are required to account for cloud and precipitation contamination.

Within the operational ARPEGE model, the cloud screening of 183.31 GHz brightness temperatures from AMSU-B/MHS is based on the 89 GHz window channel; over Europe and during the period of interest, approximately 90 % of the 183.31 GHz observations pass the cloud detection. For hyperspectral IR observations like IASI, the cloud detection is based on a more sophisticated technique than a one-channel based quality control, and allows the assimilation of channels of the instrument that are insensitive to temperature and humidity below an identified cloud layer (McNally and Watts, 2003).

For the synthetic radiances of the IRS and the MWGEO instruments, a cloud screening algorithm has been implemented in order to screen the synthetic observations contaminated by clouds and mimic the effect of the methods used with real observations. For each instrument, relevant predictors, based on hydrometeor contents of the NR, are chosen as proxies of the presence of clouds:

- For the MWGEO instrument, the total cloud ice water path (CIWP) is used as predictor for cloud screening. Indeed, 183.31 GHz microwave channels are mainly sensitive to solid hydrometeors (e.g. Hong *et al.*, 2005). The six MWGEO channels are all rejected when the CIWP exceeds a given predefined threshold. Rejecting the six channels at once mimics the cloud screening of SAPHIR data within the ARPEGE 4D-Var assimilation system (Chambon *et al.*, 2015) which rejects all channels depending on the ice scattering signature in SAPHIR channel 6.
- The 25 infrared channels from the IRS instrument are significantly affected by both liquid and solid hydrometeors so the selected proxy is an integrated cloud water + cloud ice water path (CIWP + CLWP thereafter CLCIP). This quantity is computed over three nested atmospheric layers: from model top to 300 hPa (CLCIP1), from model top to 600 hPa (CLCIP2) and from model top to the ground (CLCIP3). Then, channels mostly sensitive to the atmosphere above 300 hPa, which can be contaminated only by clouds above 300 hPa, are screened when CLCIP1 exceed a critical threshold; channels mostly sensitive to the atmosphere above 600hPa, which can be contaminated only by clouds above 600 hPa, are screened when CLCIP2 exceed a critical threshold; and channels sensitive to the surface, which can be contaminated by clouds anywhere in the atmosphere, are screened when CLCIP3 exceeds a critical threshold. This simple method mimics the more advanced "algorithm of McNally and Watts (2003)" within the OSSE framework in which the true atmosphere is known.

The four thresholds needed in this algorithm for CWIP, CLCIP1, CLCIP2 and CLCIP3, have been determined independently of the NR using the following method with the operational ARPEGE 6h forecasts: (i) the real AMSU-B/MHS and IASI observations assimilated operationally over Western Europe from July 1st to July 31st 2015 in ARPEGE have been extracted, (ii) the fraction of cloud contaminated observations have been computed for channels similar to the ones considered in the OSSE, (iii) the threshold for each parameter is defined in order to reach the same fraction of cloud contaminated observations as with real radiances.

The results of this approach show that:

- Cloud contaminated radiances represent approximately 9 % of 183.31 GHz radiances over the period which leads to a threshold of 31.5 g m^{-2} for CIWP according to its cumulative distribution function.
- For channels mostly sensitive to the atmosphere above 300 hPa, roughly 20 % of IASI radiances are contaminated by clouds which leads to a CLCIP1 threshold of 1.3 g m^{-2}
- For channels mostly sensitive to the atmosphere above 600 hPa, roughly 38 % of IASI radiances are contaminated by clouds which leads to a CLCIP2 threshold of 1.1 g m^{-2}
- For channels sensitive to the surface, roughly 62 % of IASI radiances are contaminated by clouds which leads to a CLCIP3 threshold of 0.8 g m^{-2}

Taking into account precisely the above thresholds would not make much sense within an OSSE framework; nonetheless it provides an indication on their orders of magnitude in order to provide a reasonable cloud screening for IR and MW sensors. A conservative approach was chosen: the same threshold value of 2 g m^{-2} was selected for CLCIP1, CLCIP2 and CLCIP3, and a threshold of 30 g m^{-2} was used for the CIWP.

Figure 5 shows an example of the cloud screening impact on the MWGEO and IRS observations selection for July 3rd 2015 at 00 h UTC. One can for instance see that a cloudy region was detected in the North of France and Belgium, below 300 hPa which led to the cloud screening of microwave observations as well as IRS channels peaking below 300 hPa. Another case can be seen over Spain where the CIWP is small enough to allow MW data assimilation, but the CLCIP2 is larger than the threshold, screening out all channels peaking in the 300 hPa to 600 hPa layer and below. When the selected thresholds are applied over whole the one month experiment period, the implemented cloud screening discards roughly 30 % of IRS observations and roughly 3 % of MWGEO observations (see Figure 2). These numbers are lower than the number of screened observations in reality (e.g. 9% for microwave observations). Indeed, over a limited period of time like a one-month period and a limited area domain, there is no guarantee that clouds/storms occur at the same frequency in the NR and in reality; further investigation would be needed to validate the NR on this latter aspect. Hence the cloud screening approach only ensure that high cloud amounts that would be filtered out in reality are filtered in the OSSEs as well.

For all other observations, the regular “first-guess checks” quality control is applied as in the case for real observations.

3. Experimental set up and verification methods

3.1 Experimental set up

During a so-called "spin-up period", the NR drifts from the "real" atmospheric state toward the model climatology. In order to avoid contaminating the OSSEs with the initial conditions, the first month of the NR was excluded from the experiments (see Section 2.4). Hence, data assimilation experiments have been performed from July 1st to July 31st 2015 over the AROME France domain area. A 3D-Var analysis is performed every hour, followed by a 1 h forecast that is used as background for the next analysis. A set of longer-range forecasts of +42 h is performed daily at 00 h UTC. Table 4 summarizes the set of assimilation experiments that have been undertaken.

The "CONTROL" experiment allows us to evaluate the impact of an IR multi-channels geostationary instrument added to the current observing system as well as the impact of the cloud screening. This experiment is used as a baseline to assess the impact of a GEO microwave sounder on AROME analyses and forecasts and the effect of neglecting cloud screening.

For each experiment, the NR hourly archives are used to provide the lateral boundary conditions of the AROME model.

3.2 Verification methods

Since both IRS and MWGEO channels were selected with a focus on water vapour, verifications presented below examine observing system impacts on relative humidity and precipitation forecasts.

3.2.1 Relative humidity scores

To compare the forecast skill of the different experiments, root mean square errors (RMSE) over the full AROME domain of the relative humidity between each +42 h forecast and the NR have been calculated for each forecast hour and at various pressure levels. Differences between the RH RMSE of two experiments are then averaged over the one-month period, and a confidence interval at 99 % is computed in order to highlight the

most significant differences between experiments. The latter confidence intervals are computed using Student's t-test for the mean differences at the 99 % confidence level and inflated by a factor of 1.07 to account for correlations between the daily +42 h forecasts (Geer, 2015). In Section 4, only differences between experiments which are significant at the 99 % level are taken into account in drawing the conclusions of this paper.

Figure 6 shows an example of the CURRENT experiment mean RH RMSE as well as the same scores for operational AROME forecasts with respect to the ECMWF analyses. Despite some small magnitude differences, these results show that the OSSE forecasts are characterized by relative humidity errors comparable to those of forecasts of the operational AROME model. This is an important validation of the OSSE system.

3.2.2 Precipitation scores

The precipitation forecast evaluation needs a different approach than the one described for relative humidity. Indeed model forecasts are usually characterized by mislocated precipitating events with respect to observations. Hence, point-to-point evaluations are replaced by fuzzy verifications. For each observation, these methods consider a best match between the observation and the forecast precipitation in a neighbourhood of the observation. Here, we apply the Fractions Skill Score (Ebert, 2008), varying both the size of the neighborhood and the critical rain intensity.

In the same way as for Relative Humidity, daily Fraction Skill Scores between precipitation forecasts from each experiment and the NR are computed over the full AROME domain and 99 % confidence level intervals are calculated in order to highlight statistically significant differences in the results.

4. Results

4.1 Enhancing the 2015-like observing system with a multi-channel IR geostationary instrument

A first comparison to consider is between the experiments CURRENT, CLOUD-FREE and CONTROL (assimilation of IRS with and without cloud contaminated radiances). This comparison characterizes the baseline used in the next section, as the CONTROL experiment is considered as the reference for the MWGEO experiments.

The relative RH RMSE differences (Figure 7a) reveal that assimilating 25 IRS water vapour channels in addition to current (2015) observations, without cloud screening, has a large positive impact on forecast scores. The significant benefits (at the 99 % level of confidence) spread up to the +15 h forecast lead time and range up to 12 % of relative improvement below 250 hPa and up to 20 % above 200 hPa.

As the cloud screening method described in Section 2.5 significantly reduces the number of assimilated IRS radiances, this more realistic scenario is expected to have reduced impact. Figure 7b shows that it is indeed the case, roughly by a factor of 30 % compared to the CLOUD-FREE experiment without cloud screening. This comparison hence provides results with the updated methodology compared to the one used in Guedj et al. (2014) without cloud screening. However, the CONTROL experiment is still characterized by better relative humidity forecasts than the CURRENT, up to a +18 h forecast lead time.

In both Figure 7a and 7b, the significant positive impacts do not extend beyond the +18 h forecast range. This is anticipated as limited area model forecasts tend to be driven by the lateral boundary conditions, typically beyond +12 h (e.g. Seity et al., 2011).

The IRS instrument will have a much larger set of channels than what is considered in this paper. However, further optimizations of the IRS data assimilation are beyond the scope of the present work. Indeed, as mentioned in the introduction, the configuration chosen for the assimilation of IRS radiances is taken from Guedj *et al*. (2014), with the addition of cloud screening. This preliminary configuration is likely to evolve when IRS observations are available and these optimizations are left for future work with real MTG data. Nevertheless, it was shown that the CONTROL experiment, with cloud screening, provides better forecasts than the CURRENT, and is considered as the baseline to which added MWGEO instruments with different observation errors are assimilated.

4.2 Enhancing the 2021-like observing system with a GEO microwave sounder

As explained above, the assessment of the potential impact of a GEO microwave sounder should be performed in the context of a denser observing system than the present day global observing system. Therefore the CONTROL experiment, with cloud screening, which simulates a 2021-like observing system over Europe is used as the reference experiment for the GEO microwave sounder experiments. The impact of incrementing the

CONTROL experiments with MWGEO observations is shown in Figure 8 for three different observation error magnitudes (Table 4). The three MWGEO instruments lead to significant positive benefits in terms of relative humidity forecast scores, but with different magnitudes and up to different forecast ranges:

- As shown in Figure 8a, the MWGEO with the best observation error (1.25 K standard deviation) improves relative humidity forecasts up to the +3 to +9 h forecast range. The RMSE decrease reaches 10 % between 400 and 250 hPa and more than 16 % above 200 hPa.
- With an observation error of 2.5 K (Figure 8b), the statistically significant benefits of the MWGEO still spread up to a +3 to +6 h forecast range but the magnitude is reduced to 6 % at the beginning of the forecast between 450 and 350 hPa.
- With an observation error of 5 K (Figure 8c), the statistically significant benefits are drastically reduced to a maximum of 2 to 4 % and only affect the first two forecast hours, at high altitude between 450 hPa and 150 hPa.

Since most of the MWGEO RH benefits are located above the lower troposphere, precipitation forecasts are not likely to be improved. The Fraction Skill Scores (FSS) compared to the NR on 12 h accumulated precipitation forecasts are shown in Figure 9, for the first 12 hours of the daily long forecasts, and the following 12 hours ("+24 h range" - "+12 h range"). Figure 9a and 9c show that with a 40 km neighbourhood used for the FSS computation, very little differences can be found between all the experiments described in this paper and none of them are statistically significant at the 99 % confidence level. The same conclusions can be drawn with a larger neighbourhood of 120 km (Figure 9b and 9d) as well as other neighbourhood sizes (2.5 km, 10 km, 20 km, 80 km, not shown). A much longer period of study might obtain statistically significant rainfall forecasts results.

5. Summary and concluding remarks

The objective of this study is to provide preliminary results on the potential impact of a microwave sounder at 183.31 GHz on-board a geostationary platform. The OSSEs conducted for summer mid-latitudes have been performed in several steps:

- Nature Run: a 2-month long and uninterrupted forecast, obtained from the global hydrostatic Météo-France model ARPEGE, with a daily sea surface temperature forcing using OSTIA analyses, is taken to be the “truth”.

- Synthetic observations: a full set of observations with different observation types have been simulated and calibrated with an iterative procedure in order to obtain first guess departures similar between the OSSE framework and the real AROME data assimilation system.
- New radiances from two instrument types on-board a geostationary satellite have been simulated from the NR. The observations from a GEO hyperspectral infrared sounder (IRS-like instrument) as well as a GEO microwave sounder, the latter with three different observation error magnitudes were simulated and assimilated in the OSSE experiments.
- Cloud screening: in order to preserve a realistic ratio of cloud-screened data between the new infrared and microwave instruments, a cloud screening methodology based on hydrometeor content from the NR was implemented.
- Data assimilation: several 1-month long OSSEs produced analyses and forecasts for different observing systems configurations, using the 3D-Var data assimilation system of the Météo-France convective scale limited area model AROME.
- Forecast verification: forecast scores were computed for relative humidity and precipitation, which are critical metrics for analyzing the potential impact of the new instruments.

The main findings of this study, that are significant at the 99 % confidence level, are as follows:

- Clouds have a large impact on the OSSE assimilation results for the IRS-like instrument. Compared to clear radiances, cloud roughly reduces the impacts found on relative humidity forecasts by 30 %.
- Even when accounting for cloudiness, the assimilation of 25 water vapour IRS channels provides positive impacts up to a forecast lead time of 18h with respect to a 2015-like observing system.
- The assimilation of a MWGEO instrument with 6 channels around 183.31 GHz could lead to positive impacts, even in a dense environment as the 2021-like observing system simulated in this study. However, these positive impacts strongly depend on the observation error of this potential instrument.
- A MWGEO, with observations as accurate as the ones provided by LEO satellites, brings information that propagates positively within the forecasts up to a +3 to +6 h forecast lead time.
- A MWGEO, with observations four times less accurate (5 K observation error) than the ones provided by LEO satellites, adds value to a 2021-like observing system, only to a few pressure levels, and only over the first two forecast hours.

Overall, one of the main conclusions that can be drawn from this study is that fine-scale numerical weather prediction systems do need not only observations that are frequent in space and time, but that are characterized by small observation errors as well.

As it is often the case in OSSEs, the framework used in this study suffers from a number of limitations. Some of these limitations have effects that may be anticipated:

- With more data in the CURRENT configuration, additional types of data such as from the IRS or a MWGEO are less likely to have a significant positive impact. In particular, our system does not include the assimilation of radar reflectivities, yet these data have been shown to improve AROME rainfall forecasts (Wattrelot et al., 2014).
- With more data in the CONTROL configuration, MWGEO observations are also less likely to have a significant positive impact. Indeed, as explained before, the IRS instrument will have a much larger set of channels than what is considered in this study. Furthermore, no Level 2 data derived from the IRS instrument such as Atmospheric Motion Vectors product were considered either. It is likely that assimilating more channels and more derived products from the IRS would also reduce the significant positive impact of a MWGEO.
- The cloud screening method has only been implemented for the observing systems providing the largest number of observations in the OSSEs, the IRS and the GEO microwave sounder; this means that unrealistically good other IR and MW radiances are assimilated in the OSSEs. This limitation is likely to have attenuated the impact of a MWGEO.

Other limitations may also impact the results, but their respective effects are harder to predict than the ones mentioned above:

- The experiments have been conducted over a summer period. An extension to a winter period would evaluate if the results are applicable for different seasons. The period of time considered for evaluating the impact is short (one-month), which is why a high level of confidence was selected for analysing the present results (99% plus an additional inflation factor). Extending the results with experiments over longer periods would be a useful extension of this work.
- Regarding the data assimilation system, the study used a 1h-cycle 3D-Var system with clear-sky assimilation capability. The results are hence applicable to similar systems only. Further study would of course be needed to complement these results, for instance with a 4D data assimilation system having

"all-sky" assimilation capabilities (e.g. Geer and Baordo, 2014), which may benefit more from frequent microwave observations.

- Perfect lateral boundary conditions and perfect sea surface temperature have been used. In the real world, errors on both quantities would enhance the differences between the AROME forecasts and the true atmospheric state. The impact of these assumptions may be studied by selecting other boundary conditions (e.g. from a global OSSE as in Atlas et al., 2015) and sea surface temperature conditions; this would also be an interesting extension of the present study.
- The synthetic AMV data have not been computed at the location of clouds in the NR but at the location of real AMV data. Depending on the meteorological situation, this may increase or decrease the number of AMV data in the OSSEs with respect to reality.
- Gaussian random and uncorrelated perturbations have been used to simulate observation errors but in reality there are correlated observation errors and the data assimilation system used here does not handle them correctly. Spatial resolution of the observations from the various instruments have not been considered either in this study; taking into account the higher resolution of infrared radiances (~5 km) with respect to microwave radiances (25 to 50 km) from geostationary platforms could be an interesting aspect to consider for future OSSEs at convective scale. Especially with the upcoming MTG-IRS instrument, future research on the horizontal observation error correlations will be needed in order to reduce or eliminate the spatial thinning that is currently applied.

Regarding the GEO microwave sounder concept, the characteristics of such an observing system result from a complex instrumental trade-off. The results presented in this paper suggest that if the requirement of low observation errors cannot be met, impacts on meso-scale NWP are likely to be very limited and the scientific objectives of such a mission shall for instance be focused more on nowcasting applications. Other observing system concepts may also offer the capability to bring high-revisit microwave observations with more cost-effective approaches. For example, constellations of LEO nano-satellites (e.g. the TROPICS constellation of 12 cubesats) could provide full tropical coverage every 30 minutes (see https://tropics.ll.mit.edu). Hence, as the global observing systems continues to evolve, the cost/benefit ratio for a useful GEO microwave sounder may continue to exceed available resources.

6. Acknowledgements

This study was funded by the ESA/ESTEC Contract Nr. 4000113023/13/NL/MV. The authors thank Dr Paul Ingmann for his support and guidance. Pascal Brunel provided the RTTOV coefficients for the IRS instrument. The authors thank the two anonymous reviewers who greatly helped to improve the manuscript.

7. References

Austerberry D, Gaier T, Kangaslahti P, Lambrigtsen B, McKague D, Ramos I, Ruf C, Tanner A. 2015. Test methodology for the geostar correlator. In *Geoscience and Remote Sensing Symposium (IGARSS), 2015 IEEE International (pp. 3473-3476).* IEEE. DOI:10.1109/IGARSS.2015.7326568

Atlas R, Hoffman RN, Ma Z, Emmitt GD, Wood SA, Greco S, Tucker S, Bucci L, Annane B, Hardesty RM, Murillo S. 2015. Observing System Simulation Experiments (OSSEs) to Evaluate the Potential Impact of an Optical Autocovariance Wind Lidar (OAWL) on Numerical Weather Prediction. *J. of Atm. and Oceanic Technology*, **32**(9), 1593-1613. DOI: 10.1175/JTECH-D-15-0038.1

Blackwell WJ, Bickmeier LJ, Leslie RV, Pieper ML, Samra JE, Surussavadee C, Upham CA. 2011. Hyperspectral Microwave Atmospheric Sounding. *Geoscience and Remote Sensing*, IEEE Transactions on, **49**(1), 128-142. DOI: 10.1109/TGRS.2010.2052260

Bougeault P. 1985. A simple parameterization of the large-scale effects of cumulus convection. *Mon. Wea. Rev.*, **113**(12), 2108-2121. DOI: 10.1175/1520-0493(1985)113<2108:ASPOTL>2.0.CO;2

Bizzarri B. 2000. *MW/Sub-mm sounding from geostationary orbit*. Report to EUMETSAT Science W.G., EUM/STG/SWG/9/00/DOC/11, pp.11.

Bizzarri B, Mugnai A. 2002. Requirements and perspectives for MW/sub-mm sounding from geostationary satellite. In *EUMETSAT Meteorological Satellite Conference (pp. 97-105)*.

Boukabara SA, Moradi I, Atlas R, Casey SP, Cucurull L, Hoffman RN, Ide K, Kumar VK, Li R, Li Z, Masutani M, Shahroudi N, Woollen J, Zhou Y. 2016. Community Global Observing

System Simulation Experiment (OSSE) Package:: CGOP. Description and Usage. *J. of Atm. and Oceanic Technology*. DOI: 10.1175/JTECH-D-16-0012.1

Brousseau P, Seity Y, Ricard D, Léger J. 2016. Improvement of the forecast of convective activity from the AROME□France system. *Q. J. R. Meteorol. Soc*. DOI: 10.1002/qj.2822

Bubnová R, Hello G, Bénard P, Geleyn JF. 1995. Integration of the fully elastic equations cast in the hydrostatic pressure terrain-following coordinate in the framework of the ARPEGE/Aladin NWP system. *Mon. Wea. Rev*. **123**(2), 515-535. DOI: 10.1175/1520-0493(1995)123<0515:IOTFEE>2.0.CO;2

Camps A, Park H, Bandeiras J, Barbosa J, Sousa A, d'Addio S, Martin-Neira M. 2016a. Microwave Imaging Radiometers by Aperture Synthesis-Performance Simulator (Part 1): Radiative Transfer Module. *J. Imaging* **2**(2), 17. doi:10.3390/jimaging2020017

Camps A, Park H, Kang Y, Bandeiras J, Barbosa J, Vieira P, Friaças A, d'Addio S. 2016b. Microwave Imaging Radiometers by Aperture Synthesis Performance Simulator (Part 2): Instrument Modeling, Calibration, and Image Reconstruction Algorithms. *J. Imaging* **2**(2), 18. doi:10.3390/jimaging2020018

Carlström A, Christensen J, Embretsen J, Emrich A, De Maagt P. 2009. A Geostationary Atmospheric Sounder for now-casting and short-range weather forecasting. In *Antennas and Propagation Society International Symposium. APSURSI'09. IEEE (pp. 1-4)*. IEEE. DOI:10.1109/APS.2009.5172067

Caumont O, Ducrocq V, Delrieu G, Gosset M, Pinty JP, Parent du Châtelet J, Andrieu H, Lemaître Y, Scialom G. 2006. A radar simulator for high-resolution nonhydrostatic models. Journal of Atmospheric and Oceanic Technology. **23**(8). 1049-1067. DOI: 10.1175/JTECH1905.1

Chambon P, Meunier LF, Guillaume F, Piriou JM, Roca R, Mahfouf JF. 2015. Investigating the impact of the water‐vapour sounding observations from SAPHIR on board Megha‐Tropiques for the ARPEGE global model. *Q.J.R. Meteorol. Soc*., **141**(690): 1769-1779. DOI: 10.1002/qj.2478

Chen K, Gasiewski AJ, Zhang K, Guo W, Li Q. 2015. Simulation of imaging technology for geostationary passive microwave observation. In *Geoscience and Remote Sensing Symposium (IGARSS), 2015 IEEE International (pp. 4871-4874)*. IEEE. DOI: 10.1109/IGARSS.2015.7326922

Christensen J, Carlström A, Ekström H, Emrich A, Embretsén J, De Maagt, P, Colliander A. 2007. GAS: The geostationary atmospheric sounder. In *Geoscience and Remote Sensing Symposium (IGARSS), 2007 IEEE International (pp. 223-226).* IEEE. doi: 10.1109/IGARSS.2007.4422770

Courtier P, Freydier C, Geleyn JF, Rabier F, Rochas M. 1991. The ARPEGE project at Meteo-France. In *ECMWF Seminar Proceedings* (Vol. 2, pp. 193-231).

Courtier P, Geleyn JF. 1988. A global numerical weather prediction model with variable resolution: Application to the shallow-water equations. *Q.J.R. Meteorol. Soc.*, **114**(483). 1321-1346. DOI: 10.1002/qj.49711448309

El-Raey M. 1982. Remote sensing of atmospheric waves in O2 and H2O microwave emissions. *Radio Science*, **17**(04), 766-772. doi: 10.1029/RS017i004p00766

Errico RM, Yang R, Masutani M, Woollen J. 2007. The use of an OSSE to estimate characteristics of analysis error. *Meteorologische Zeitschrift* **16**(6), 695-708, DOI:10.1127/0941-2948/2007/0242

Errico RM., Yang R, Privé NC, Tai KS, Todling R., Sienkiewicz ME, Guo J. 2013. Development and validation of observing-system simulation experiments at NASA's Global Modeling and Assimilation Office. *Q.J.R. Meteorol. Soc*., **139,** 1162–1178. doi: 10.1002/qj.2027

Gaier T, Lambrigtsen B, Kangaslahti P, Lim B, Tanner A, Harding D, Owen H, Soria M, O'Dwyer I, Ruf C, Miller R, Block B, Flynn M, Whitaker S. 2011. GeoSTAR-II: A prototype water vapor imager/sounder for the PATH mission. In *Geoscience and Remote Sensing Symposium (IGARSS), 2011 IEEE International. (pp 3626-3628), doi: 10.1109/IGARSS.2011.6050009*

Gasiewski AJ, Voronovich A, Weber BL, Stankov B, Klein M, Hill RJ, Bao JW. 2003. Geosynchronous microwave (GEM) sounder/imager observation system simulation. In *Geoscience and Remote Sensing Symposium, IGARSS'03. Proceedings. 2003 IEEE International (Vol. 2, pp. 1209-1211).* IEEE.

Geer AJ, Baordo F. 2014. Improved scattering radiative transfer for frozen hydrometeors at microwave frequencies. *Atmospheric Measurement Techniques*, **7**(6), 1839-1860. DOI: 10.5194/amt-7-1839-2014

Geer A. 2015. *Significance of changes in medium-range forecast scores*. ECMWF Technical Memorandum, No. 766.

Guedj S, Guidard V, Ménétrier B, Mahfouf JF, Rabier F. 2014. *Future benefits of high-density radiance data from MTG-IRS in the AROME fine-scale forecast model*. Final Report. Eumetsat Fellowship report, Météo-France & CNRS/CNRM-GAME. (https://hal-meteofrance.archives-ouvertes.fr/meteo-01133380)

Hoffman RN, Atlas R. 2015. Future Observing System Simulation Experiments. *Bull. Am Meteorol. Soc.* DOI: 10.1175/BAMS-D-15-00200.1

Hong G, Heygster G, Miao J, Kunzi K. 2005. Detection of tropical deep convective clouds from AMSU-B water vapor channels measurements. *J. Geophys. Res. Atmos.,* **110**(D5). DOI: 10.1029/2004JD004949

Lambrigtsen B, Tanner A, Gaier T, Kangaslahti P, Brown S. 2007. Prototyping GeoSTAR for the PATH mission. In P*roceedings NASA Science Technology Conference (pp. 19-21).* University of Maryland University College, Adelphi, MD, USA

Li Q, Chen K, Guo W, Li Y, Dou H. 2015. Rotating mirrored aperture synthesis (RMAS) for passive microwave remote sensing. In *Geoscience and Remote Sensing Symposium (IGARSS), 2015 IEEE International (pp. 3481-3484)*. IEEE. DOI: 10.1109/IGARSS.2015.7326570

Liu H, Wu J, Zhang S, Yan J, Zhang C, Sun W, Niu L. 2009. Conceptual Design and Breadboarding Activities of Geostationary Interferometric Microwave Sounder (GIMS). In

Geoscience and Remote Sensing Symposium (IGARSS), 2009 IEEE International (pp. 1039-1042). IEEE. Doi: 10.1109/IGARSS.2009.5417956

Liu H, Wu J, Zhang S, Yan J, Niu L, Zhang C, Sun W, Li H, Li B. 2011. The geostationary interferometric microwave sounder (GIMS): instrument overview and recent progress. In *Geoscience and Remote Sensing Symposium (IGARSS), 2011 IEEE International (pp. 3629-3632)*. IEEE. Doi: 10.1109/IGARSS.2011.6050010

Ma Z, Riishøjgaard LP, Masutani M, Woollen JS, Emmitt GD. 2015. Impact of different satellite Wind Lidar Telescope configurations on NCEP GFS forecast skill in observing system simulation experiments. *J. Atm. and Oceanic Technology*, **32**(3), 478-495. DOI: 10.1175/JTECH-D-14-00057.1

Martín-Neira M, LeVine DM, Kerr Y, Skou N, Peichl M, Camps A, Corbella I, Hallikainen M, Font J, Wu J, Mecklenburg S, Drusch M. 2014. Microwave interferometric radiometry in remote sensing: An invited historical review. *Radio Sci.*, **49**, 415–449, doi:10.1002/2013RS005230.

Masutani M, Schlatter TW, Errico RM, Stoffelen A, Andersson E, Lahoz W, Woollen JS, Emmitt GD, Riishøjgaard LP, Lord SJ. 2010. Observing system simulation experiments. In *Data Assimilation* (pp. 647-679). Springer Berlin Heidelberg.

McNally AP, Watts PD. 2003. A cloud detection algorithm for high-spectral-resolution infrared sounders. *Q.J.R. Meteorol. Soc.* **129**: 3411-3423. doi: 10.1256/qj.02.208

McCarty W, Errico RM, Gelaro R. 2012. Cloud coverage in the joint OSSE nature run. *Mon. Wea. Rev*. **140**(6), 1863-1871. DOI: 10.1175/MWR-D-11-00131.1

Prigent C, Pardo JR, Rossow WB. 2006. Comparisons of the millimeter and submillimeter bands for atmospheric temperature and water vapor soundings for clear and cloudy skies. *Journal of Applied Meteorology and climatology*. **45**(12), 1622-1633. DOI: 10.1175/JAM2438.1

Privé NC, Errico RM, Tai KS. 2013a. Validation of the forecast skill of the Global Modeling and Assimilation Office Observing System Simulation Experiment. *Q.J.R. Meteorol. Soc*. **139**: 1354-1363. doi: 10.1002/qj.2029

Privé NC, Xie Y, Woollen J, Koch S, Atlas R, Hood R. 2013b. Evaluation of the Earth Systems Research Laboratory's global Observing System Simulation Experiment system. *Tellus* A, **65**. doi:http://dx.doi.org/10.3402/tellusa.v65i0.19011

Privé NC, Xie Y, Koch S, Atlas R, Majumdar SJ, Hoffman RN. 2014. An Observing System Simulation Experiment for the Unmanned Aircraft System Data Impact on Tropical Cyclone Track Forecasts. *Mon. Wea. Rev.* **142**(11), 4357-4363. DOI: 10.1175/MWR-D-14-00197.1

Rodriguez A, Stuhlmann R, Tjemkes S, Aminou DM, Stark H, Blythe P. 2009. Meteosat Third Generation (MTG): Mission and System Concepts. *Proc. SPIE* 7453, Infrared Spaceborne Remote Sensing and Instrumentation XVII, 74530C (September 01, 2009); doi:10.1117/12.824236

Seity Y, Brousseau P, Malardel S, Hello G, Bénard P, Bouttier F, Lac C, Masson V. 2011. The AROME-France convective-scale operational model. *Mon. Wea. Rev.* **139**(3), 976-991.

Stark JD, Donlon CJ, Martin MJ, McCulloch ME. 2007. OSTIA: An operational, high resolution, real time, global sea surface temperature analysis system. In *Oceans 2007-Europe (pp. 1-4)*. IEEE. DOI: 10.1109/OCEANSE.2007.4302251

Stuhlmann R, Rodriguez A, Tjemkes S, Grandell J, Arriaga A, Bézy JL, Aminou D, Bensi P. 2005. Plans for EUMETSAT's Third Generation Meteosat geostationary satellite programme. *Advances in Space Research* **36**(5), 975-981. DOI: 10.1016/j.asr.2005.03.091

Wang H, Huang XY, Chen Y. 2013. An observing system simulation experiment for the impact of MTG candidate infrared sounding mission on regional forecasts: system development and preliminary results. *ISRN Meteorology* **2013**. Article ID 971501. doi: 10.1155/2013/971501

Wattrelot E, Caumont O, Mahfouf JF. 2014. Operational implementation of the 1D+ 3D-Var assimilation method of radar reflectivity data in the AROME model. *Mon. Wea. Rev*. **142**(5), 1852-1873. DOI: 10.1175/MWR-D-13-00230.1

Zhang C, Liu H, Wu J, Zhang S, Yan J, Sun W, Li H. 2012. Imaging performance analysis for the Geostationary Interferometric Microwave Sounder (GIMS) demonstrator. In *Microwave Radiometry and Remote Sensing of the Environment (MicroRad), 12th Specialist Meeting on (pp. 1-4)*. IEEE.

Zhang Y, Liu H, Wu J, He J, Zhang C. 2015a. Target brightness temperature simulation and analysis for the geostationary interferometric microwave sounder (GIMS). In *Geoscience and Remote Sensing Symposium (IGARSS), 2015 IEEE International (pp. 3477-3480)*. IEEE. DOI: 10.1109/IGARSS.2015.7326569

Zhang C, Liu H, Wu J, Zhang S, Yan J, Niu L, Sun W, Li H. 2015b. Imaging analysis and first results of the geostationary interferometric microwave sounder demonstrator. *Geoscience and Remote Sensing*, IEEE Transactions on, **53**(1), 207-218. DOI:10.1109/TGRS.2014.2320983

Tables

Table 1: List of observing systems considered in the CURRENT experiment

Type of measurement	Instrument
Surface measurements	Surface stations, ships and buoys
	Terrestrial GPS
	Wind profilers
Altitude measurements	Radiosondes
	Aircraft measurements
Satellite measurements	Atmospheric motion vectors
	Scatterometer winds
	HIRS
	AMSU-A
	AMSU-B/MHS
	ATMS
	SSMI/S
	IASI
	SEVIRI

Table 2: IRS channels assimilated

Channel index	Central wavenumber
914	**1660.00 cm^{-1}**
946	**1680.00 cm^{-1}**
958	**1687.50 cm^{-1}**
970	**1695.00 cm^{-1}**
978	**1700.00 cm^{-1}**
990	**1707.50 cm^{-1}**
1010	**1720.00 cm^{-1}**
1036	**1736.25 cm^{-1}**
1038	**1737.50 cm^{-1}**
1124	**1791.25 cm^{-1}**
1130	**1795.00 cm^{-1}**
1142	**1802.50 cm^{-1}**
1154	**1810.00 cm^{-1}**
1156	**1811.25 cm^{-1}**
1162	**1815.00 cm^{-1}**
1172	**1821.25 cm^{-1}**
1174	**1822.50 cm^{-1}**
1176	**1823.75 cm^{-1}**
1228	**1856.25 cm^{-1}**
1260	**1876.25 cm^{-1}**
1316	**1911.25 cm^{-1}**
1360	**1938.75 cm^{-1}**
1384	**1953.75 cm^{-1}**
1400	**1963.75 cm^{-1}**
1432	**1983.75 cm^{-1}**

Table 3: Channels of a hypothetical Microwave geosounder

Channel index	Central frequency (GHz)
1	**183.31 ±0.2**
2	**183.31 ±1.1**
3	**183.31 ±2.8**
4	**183.31 ±4.2**
5	**183.31 ±6.8**
6	**183.31 ±11.0**

Table 4. List of the experiment names and observing systems specifications

Name	Description of the simulated observations used
CURRENT	**Observations of the AROME DAS (excluding radar data)**
CLOUD-FREE	**CURRENT + idealized IRS observations**
CONTROL	**CURRENT + IRS observations**
MWGEOx1	**CONTROL + MWGEO (observation error=1.25K)**
MWGEOx2	**CONTROL + MWGEO (observation error=2.5K)**
MWGEOx4	**CONTROL + MWGEO (observation error=5K)**

Figures

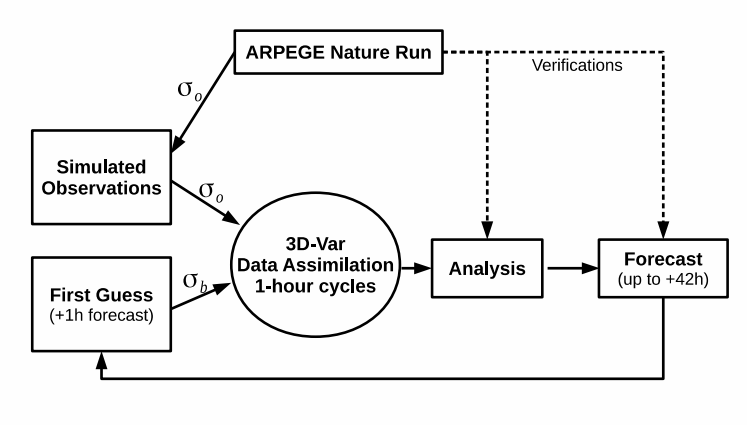

Figure 1. Observing System Simulation Experiment framework. Sigma corresponds to either observations error covariances or background error covariances.

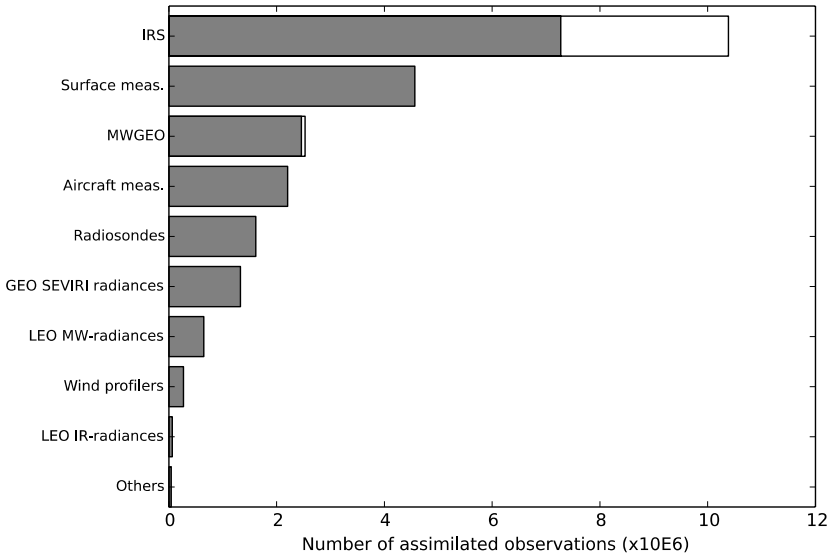

Figure 2. Number of assimilated observations from July 1st to July 31st 2015. The "surface measurements" include surfaces stations, ships buoys and terrestrial GPS observations. Satellite measurements are split between IR and MW radiances and between: Low Earth Orbit (LEO) or Geostationary Earth Orbit (GEO). The "Others" amount includes atmospheric motion vectors and scatterometer surface wind observations. For the IRS and the MWGEO observations, the filled grey rectangles are extended with not-filled rectangles corresponding to the number of observations discarded by the cloud screening.

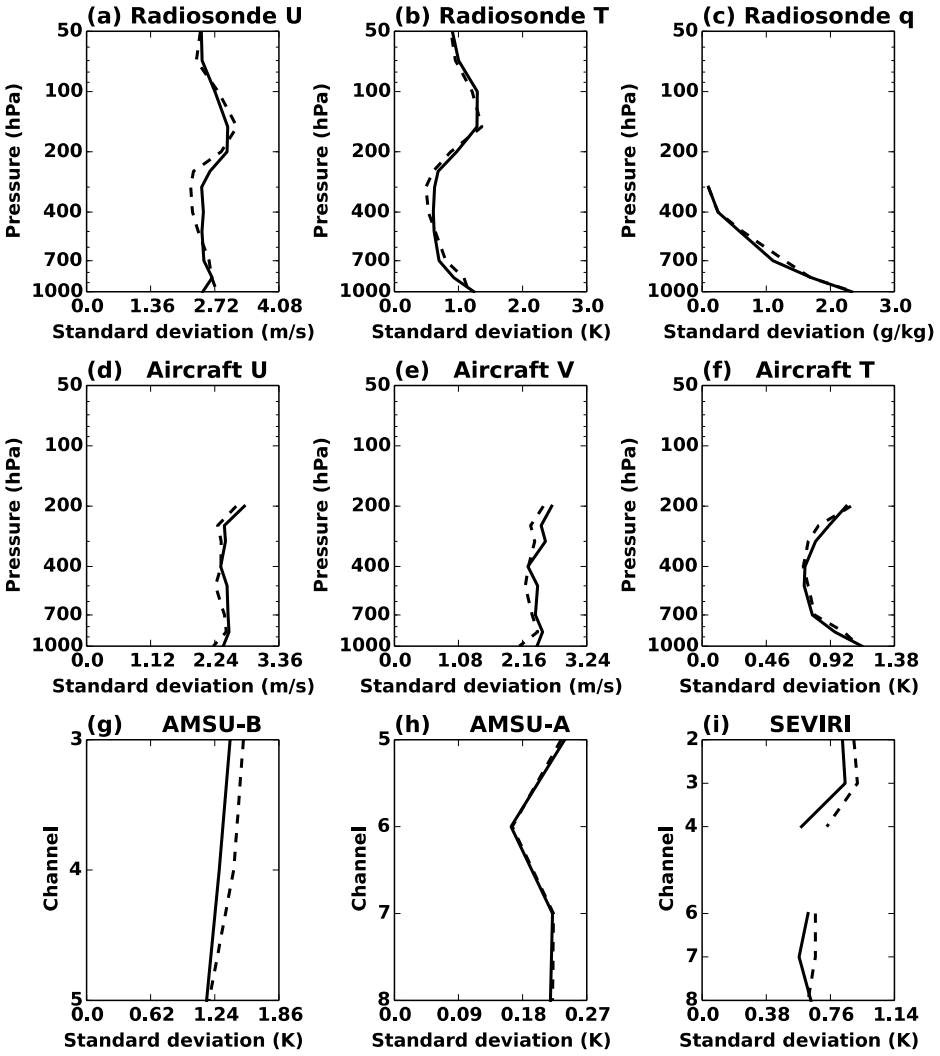

Figure 3. Standard deviations of first guess departures for radiosondes (first row), aircraft reports (second row) and satellite observations from AMSU-B/MHS, AMSU-A and SEVIRI (third row) for the calibrated OSSE (solid lines) and the operational AROME results (dashed lines). The standard deviation values have been computed over a ten-day period with one-hour assimilation cycles from July 1st to July 10th 2015 and each sample contains more than one thousand observations.

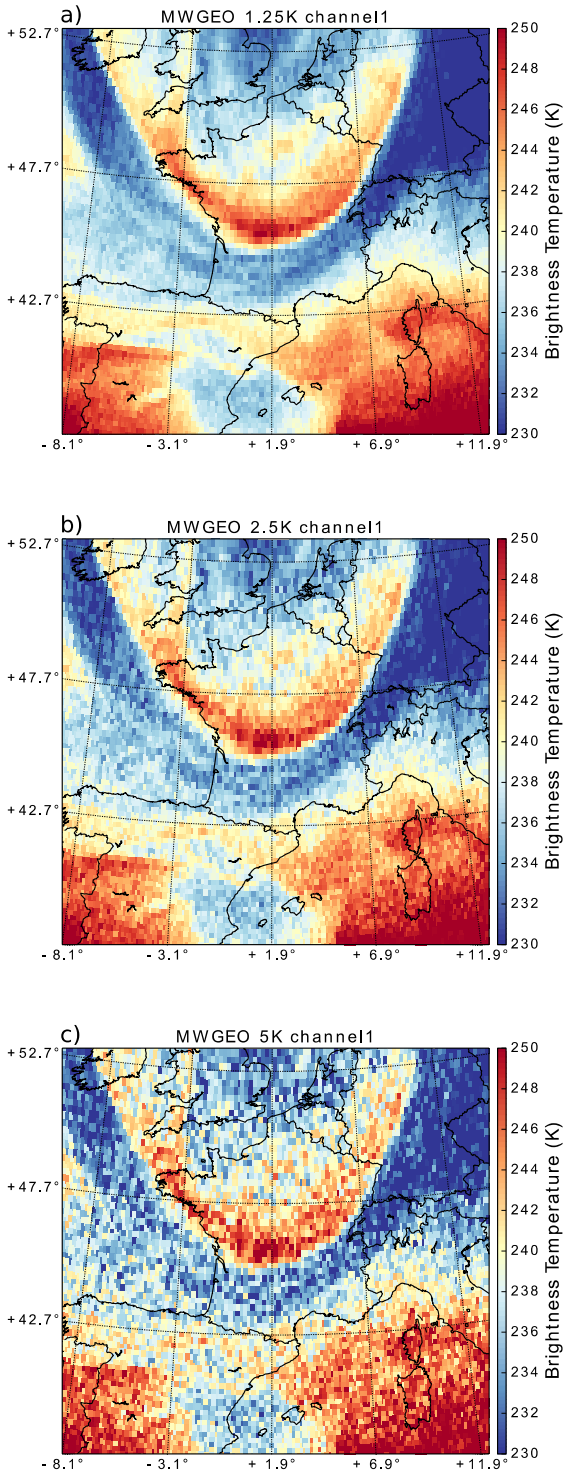

Figure 4. Simulated Brightness Temperature over the AROME domain on the MSG/SEVIRI Level 1 data grid at 183.31 ± 0.2 GHz (channel 1) for (a) MWGEOx1 (σ_o = 1.25 K), (b) MWGEOx2 (σ_o = 2.5 K) and (c) MWGEOx4 (σ_o = 5 K) for July 2nd, 2015 at 12 h UTC.

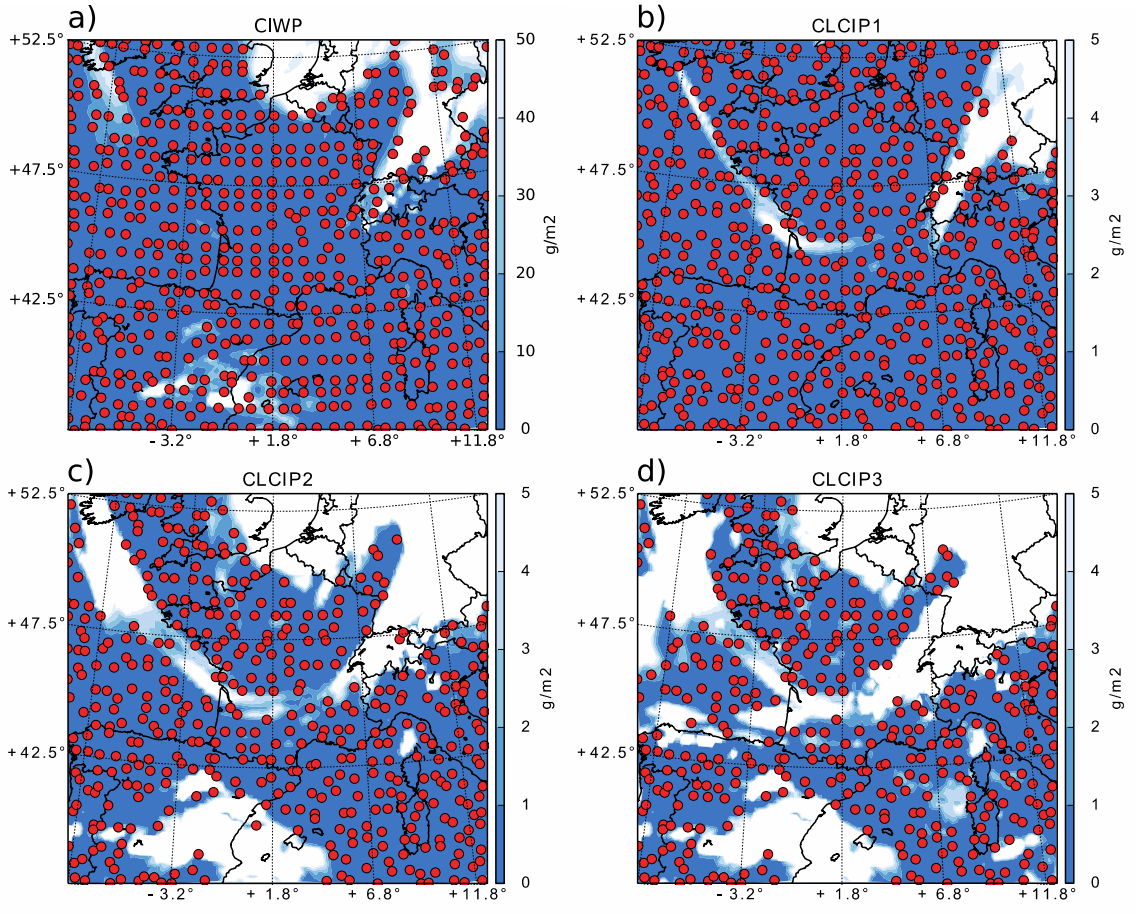

Figure 5: Example of MWGEO and IRS active observations after cloud screening (circles) for July 3rd, 2015 at 00 h UTC. (a): channel 4 of the MWGEO peaking at 550 hPa and threshold on CIWP of 30 g m^{-2}, (b) channel 978 of the IRS peaking at 150 hPa and threshold on CLCIP1 of 2 g m^{-2}, (c) channel 1130 of the IRS peaking at 350 hPa and threshold on CLCIP2 of 2 g m^{-2}, (d) channel 1260 of the IRS peaking at 600 hPa and threshold on CLCIP3 of 2 g m^{-2}. The Nature Run cloud screening parameter for each channel is plotted in background.

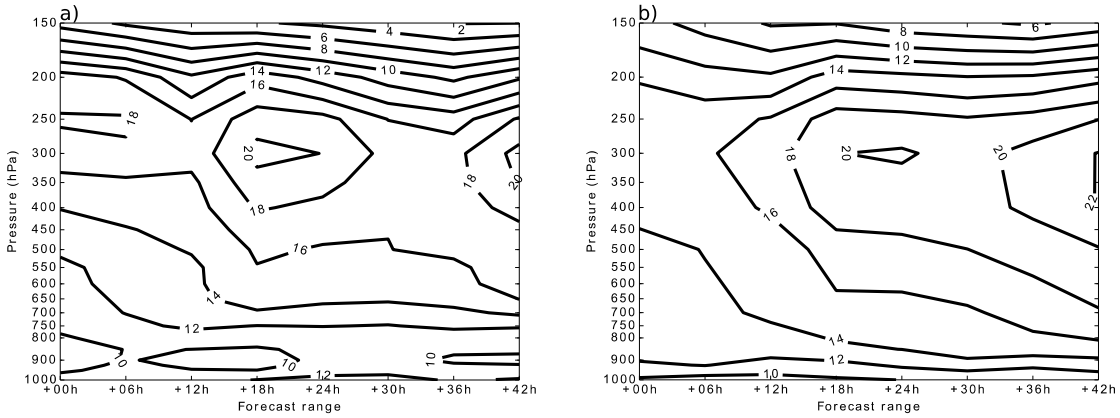

Figure 6. Relative Humidity (RH) Root Mean Square Error (RMSE) over the model domain of the CURRENT experiment with respect to the Nature Run averaged over the time period from July 1st to July 31st 2015, as a function of forecast range and pressure levels (a). Same but for operational AROME forecasts with respect to ECMWF analyses (b).

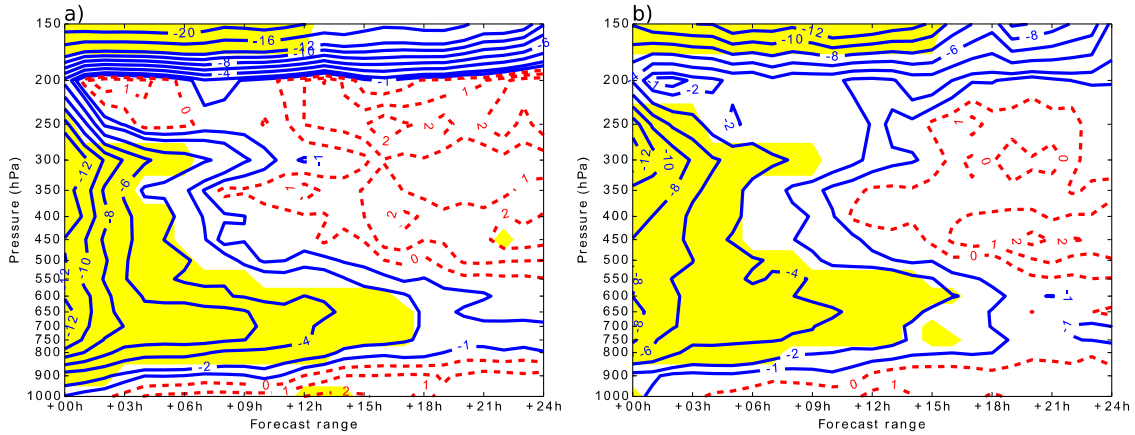

Figure 7. Difference ("CLOUD-FREE" - "CURRENT") of the RH RMSE over the AROME domain (a) and difference ("CONTROL" – "CURRENT") of the RH RMSE over the AROME domain (b) and the period from July 1st to 31st July 2015. Positive impacts of the IRS instrument correspond to negative differences of RMSE (full isolines). Filled areas indicate statistically significant results at the 99 % confidence level.

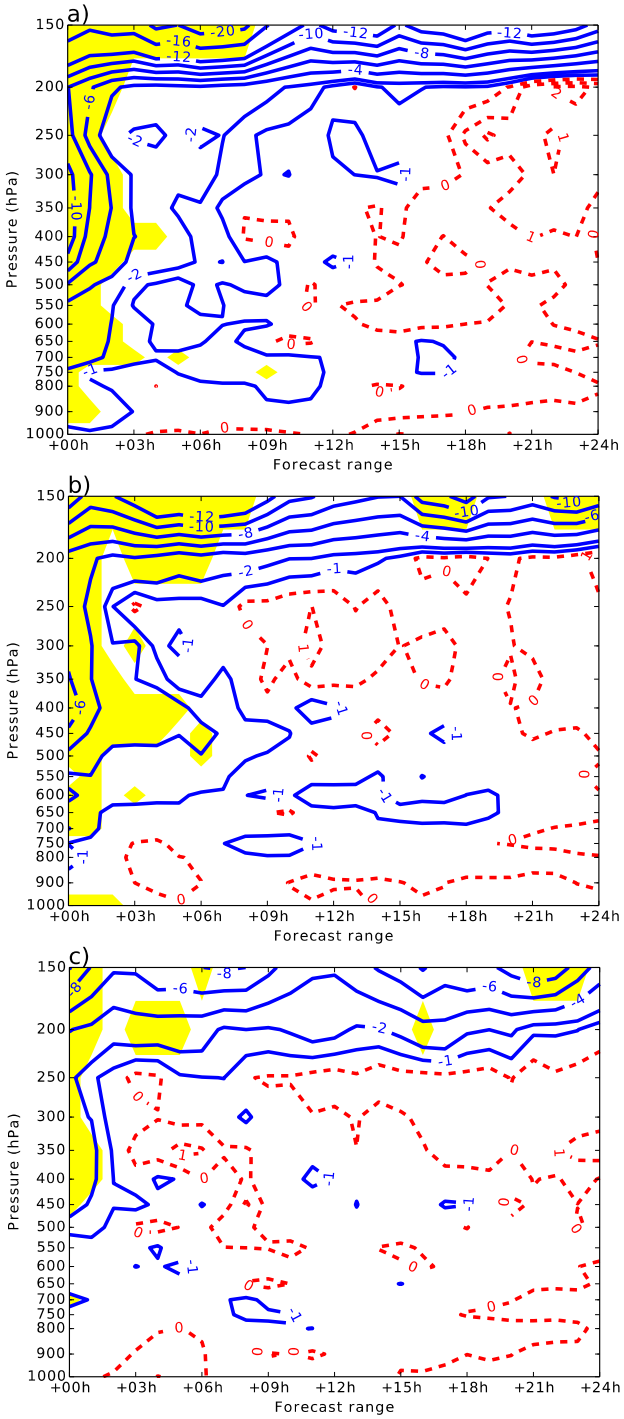

Figure 8. Same as Figure 7 but considering differences of RH RMSE over the model domain between (a) "MWGEOx1" and "CONTROL", (b) between "MWGEOx2" and "CONTROL" , and (c) between "MWGEOx4" and "CONTROL".

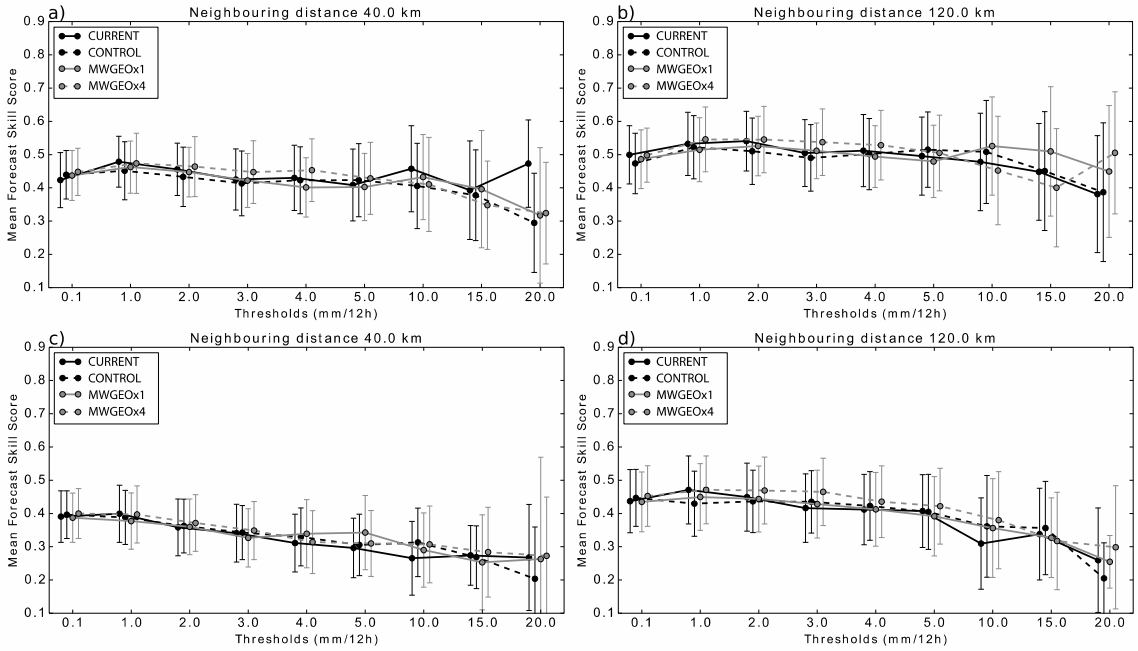

Figure 9. Mean Fractions Skill Score of the "CURRENT", "CONTROL", "MWGEOx1" and "MWGEOx4" experiments for a 40km neighborhood (a and c) and a 120km neighborhood (b and d) averaged over the time period from July 1st to 31st July 2015, as function accumulated precipitation intensities. The first row (a and b) corresponds to 12-hour accumulated rainfall forecasts between the +0h and +12h forecast ranges; the second row (c and d) corresponds to 12-hour accumulated rainfall forecasts between the +12h and +24h forecast ranges. The error bars indicate confidence intervals on the mean score at the 99 % level.